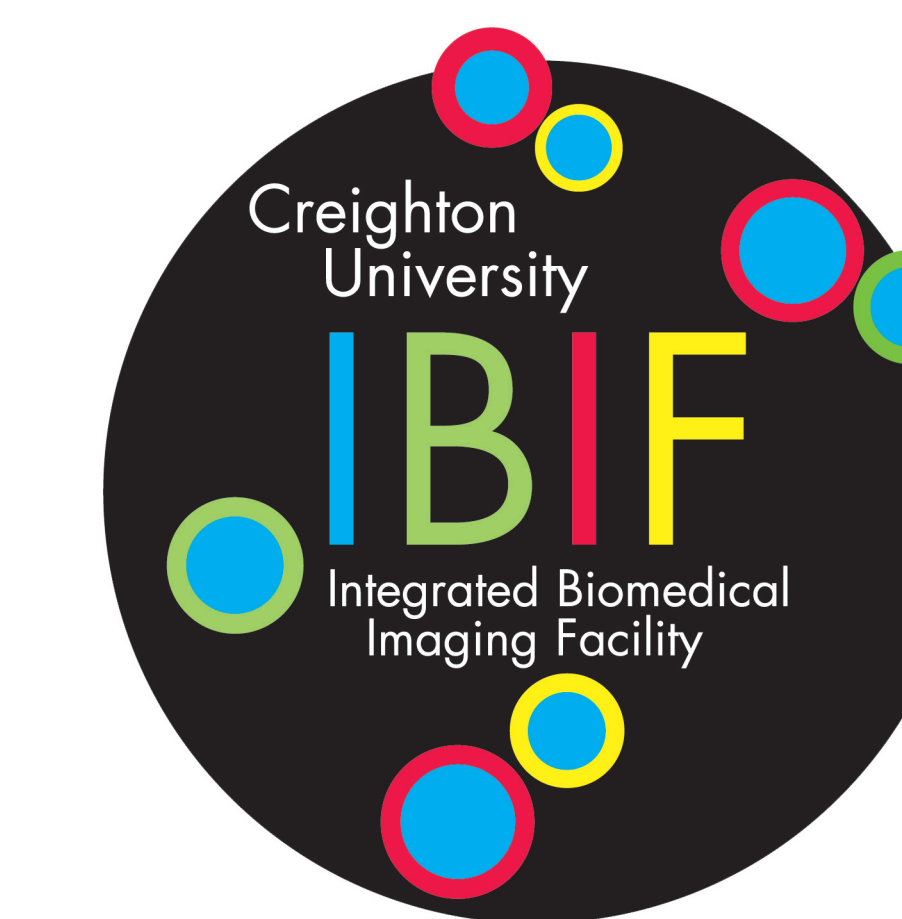


Photo- and bio-physical characterization of novel blue and near-infrared lipophilic fluorophores for neuronal tracing

Jeff Tonniges¹, Maria Hansen¹, Bernd Fritsch², Brian Gray³, Michael G. Nichols^{1,2}

Creighton University, Departments of Physics¹ and Biomedical Sciences², Omaha, NE 68178. ³Molecular Targeting Technologies, Inc. West Chester, PA 19380



Abstract

Lipophilic fluorescent dyes have been used to trace neuronal connections because of their ability to diffuse laterally between nerve cell membranes. Given the large number of connections that a typical neuron makes with its neighbors, a diffusion-matched set of spectrally distinct dyes is desirable. Previously, a trio of dyes was developed with well-separated green, red and far red fluorescence emission that permitted triple labeling [1]. To extend this set to five, we have been characterizing the properties of novel blue and near-infrared candidates. By combining two-photon and confocal microscopy all of these candidates can be imaged using a single Ti:S laser. Here we present measurements of the absolute two-photon excitation spectra along with single- and two-photon fluorescence recovery after photobleaching measurements of the diffusion coefficient in spinal cord samples.

Introduction

Novel lipophilic neurotracer probes with emission peaks in the blue (PTIR 334, 335, 336) and near infrared (PTIR 301) have been developed to complement the current set of NeuroVue dyes (Maroon, Red, and Jade) [1]. These dyes diffuse laterally along nerve cell membranes in fixed tissue, allowing tracing of the position of a given neuron within the neuronal network at various stages of development. If any of these dyes are to be a useful addition to the established set, it must be possible to efficiently excite and detect their fluorescence using conventional fluorescence imaging equipment. Furthermore, it is desirable that all of the dyes have similar lateral diffusion characteristics so they may be applied using similar protocols.

Materials and Methods

Confocal and Multiphoton Laser Scanning Microscopy

Given the well known advantages of near-infrared excitation in biological imaging, we have used the tunable output of a femtosecond Ti:S laser to excite both the near-infrared (PTIR 301, single-photon excitation (IPE) confocal) and blue (PTIR 334, 335, 336, two-photon excitation (2PE)) emitting candidate fluorophores. Images were acquired using a Zeiss 510 LSM NLO Meta microscope with dichroic and emission filters appropriately chosen (PTIR 301: excitation wavelength 720 nm, primary dichroic 80/20 beamsplitter, 785/60 emission filter (Chroma); PTIR 334, and 336: excited at 860 nm using the standard HFT KP 650 primary dichroic, NFT 545 nm secondary dichroic and a 500/40 bandpass filter.

Two-photon excitation cross section measurements

Relative two-photon action cross sections were determined with Fluorescein as reference and Lucifer Yellow as internal control, two standard fluorophores with well-characterized properties [2]. PTIR dye solutions were prepared in ethanol and placed in a sealed cuvette (Starna cells) at the focus of a 10x/0.25 NA objective. The sample was excited at wavelengths ranging from 720 - 980 nm using the apparatus described in Figure 1.

For two-photon excitation of wavelength λ , the fluorescence intensity increases quadratically with excitation laser power, $P(t)$,

$$\langle F(t) \rangle = \phi(\eta\delta) C \frac{8n}{\pi \lambda} g^{(2)} \langle P(t) \rangle^2 = A \langle P(t) \rangle^2 \quad (\text{Eq. 1})$$

where C is the concentration, δ is the two-photon cross section, η is the fluorescence quantum yield, ϕ is the detection efficiency, n is the index of refraction of the solvent, and $g^{(2)}$ is a measure of the temporal coherence of the beam. This last term depends on the pulse shape, width, and repetition rate of the laser. The action cross section, $\eta\delta$, for an unknown (U) fluorophore can be determined by measuring the variation in fluorescence count rate with average laser power relative to a known standard (K, Fluorescein),

$$(\eta\delta)_U = (\eta\delta)_K \left(\frac{n_K}{n_U} \right) \left(\frac{\phi_K}{\phi_U} \right) \left(\frac{C_K}{C_U} \right) \left(\frac{A_U}{A_K} \right) \quad (\text{Eq. 2})$$

To determine the A coefficients, the detected fluorescence intensity was fit to a second-order polynomial of the average laser power. All other parameters were independently measured.

Intercostal Nerve Injection

Preparation of Tissue. Mice used for this study were E18.5 or P0 when they were euthanized. The mothers were injected with Avertin intramuscularly for the purpose of anesthetizing the embryos, and the pups were directly anesthetized with Avertin. Both newborns and embryos were perfused with and stored in 4% paraformaldehyde (PFA) at 4°C. All breeding and euthanasia was conducted using procedures approved by the Creighton University IACUC (protocol #0630.1).

Intercostal Nerve Labeling. The intercostal nerves were prepared by completely removing all internal organs and tissue in the thoracic and abdominal cavities. A small incision was made with microscissors using an anterior approach through the ribs and intercostal muscles. The incision was parallel to and near the spinal cord, running the length of 2-4 ribs. A rectangular piece of dye labeled filter strip was cut to size and placed into the incision. After labeling, the preparation was placed into 4% PFA and incubated at 36-40°C for 24, 48, 64.5, 72, or 96 hours.

Dissection and Mounting. After the appropriate incubating time all tissue posterior to the injected intercostal spaces was dissected away including skin, superficial and deep back muscles. The labeled intercostal nerves were removed along with one unlabeled intercostal space to be used as a control. The preparation was then mounted on a glass slide with glycerol and a glass coverslip placed on top. Generally the slide was imaged immediately following dissection, but if this could not be done it was kept at 4°C until it was imaged. Note: some diffusion will occur if the sample is left for long periods of time at this temperature.

Measurements of Candidate Fluorophore Diffusion

In this study, we considered several approaches to characterizing the diffusion of the candidate fluorophores including measurements of (1) diffusion distance vs. incubation time (2) the decrease in concentration with distance along the nerve fiber, and (3) Fluorescence Recovery after Photobleaching (FRAP). Each approach is summarized briefly below.

Diffusion Distance vs. Incubation Time (Figure 3-4). Laser scanning microscopy of the labeled peripheral nerve fibers was conducted using a low-magnification 20x objective. Examples for PTIR 301, 334 and 336 are shown in Figure 3. The length of the stained portion of the nerve fiber was measured using Image J analysis software. The end of the fiber was consistently chosen at the point where the fluorescence decreased within 5 standard deviations of the background. In general, the root-mean-squared displacement is expected to increase according to:

$$\Delta x_{RMS} = 2Dt^\alpha \quad (\text{Eq. 3})$$

where the time-scaling exponent α is less than 0.5 for anomalous sub-diffusion, equal to 0.5 for Fickian diffusion, and greater than 0.5 for anomalous super-diffusion.

Spatial Decay of Dye Concentration (Figure 5). Another approach is to analyze the spatial distribution of fluorescence, tentatively assumed to be proportional to dye concentration, C . Assuming a Gaussian distribution,

$$C = Be^{-\frac{x^2}{2Dt}} \quad (\text{Eq. 4})$$

the effective diffusion coefficient is determined by a linear fit of the data, plotted as the natural log of the concentration against the square of the distance,

$$\ln(C) = \left(-\frac{1}{2Dt}\right)x^2 + b = mx^2 + b \quad (\text{Eq. 5})$$

Fluorescence Recovery after Photobleaching (Figure 6). The final method used to evaluate diffusion was to monitor the rate of recovery of fluorescence following photobleaching through repeated laser scanning of a region of the peripheral nerve fiber. Again, fluorescence intensity profiles along a line passing through the bleached region was extracted from image sequences using Image J. The spatial profiles at two successive timepoints during the recovery were fit to the numerical solution of the one-dimensional diffusion equation assuming a constant effective diffusion coefficient. The fluorescence intensity was held constant at the boundary of the photobleaching zone.

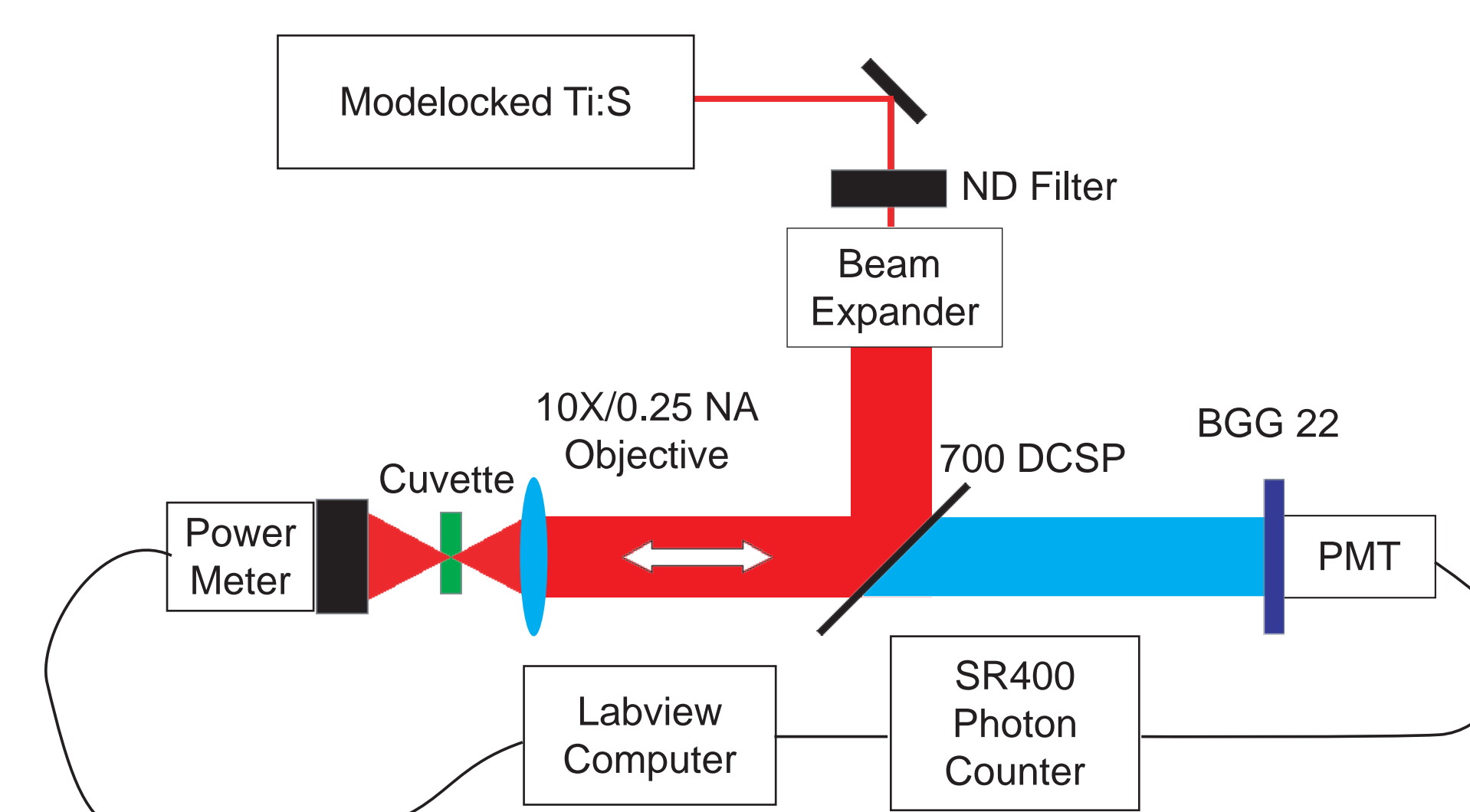


Figure 1. Apparatus used to measure two-photon action cross sections. The expanded excitation beam was reflected from the 700-nm shortpass dichroic into the objective. The resulting fluorescence was collected using the same objective, passed back through the dichroic and filtered using a BGG22 blue-glass filter before being detected by a PMT. Photon counting was performed using a SR400 photon counter controlled by LabView. For each fluorophore, the mean count rate of three trials was measured as a function of excitation laser power.

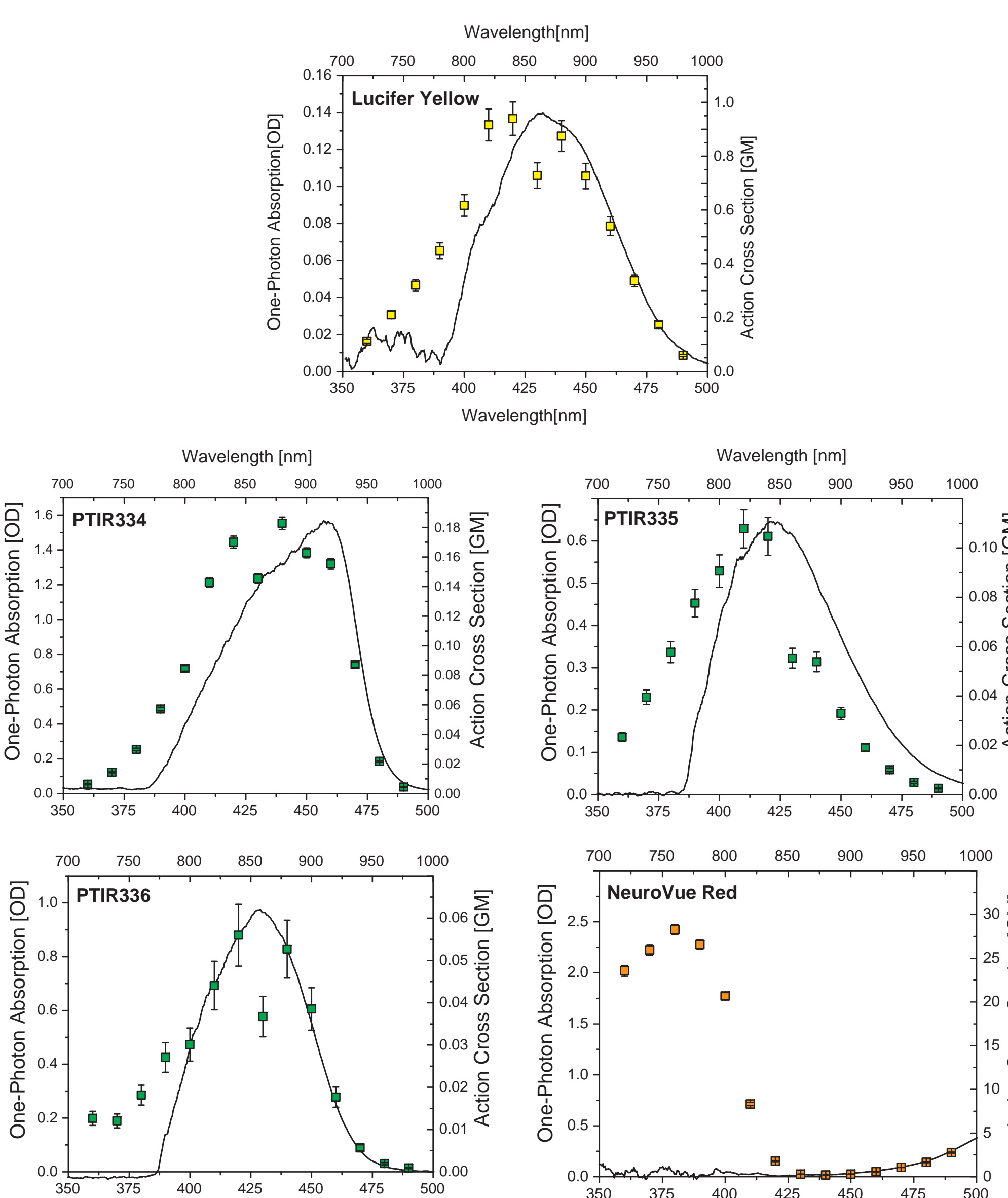


Figure 2. One- and two-photon excitation spectra for Lucifer Yellow, NeuroVue Red, and several blue candidate dyes (PTIR 334, 335 and 336). Datapoints (top and right axes) show measurements of the two-photon action cross section and errorbars represent the standard deviation. For comparison, the one-photon absorption spectra (lines, bottom and left axes) are plotted with appropriately scaled axes. All measurements were made relative to Fluorescein, while Lucifer Yellow served as an internal control. $1\text{GM} = 10^{50} \text{ cm}^2/\text{s/photon}$.

Table 1: Summary of 2PE Cross Section Measurements

	Lucifer Yellow	NeuroVue Red	PTIR 334	PTIR 335	PTIR 336
1PE Peak Wavelength	428 nm	570 nm	440 nm	406 nm	412 nm
$\sigma (\text{M}^{-1}\text{cm}^2)$	12,000	115,438	51,600	17,900	20,100
2PE Peak Wavelength	840 nm	760 nm	880 nm	820 nm	840 nm
$\eta\delta$ (GM)	0.94 ± 0.06	28.3 ± 0.6	0.183 ± 0.004	0.108 ± 0.008	0.056 ± 0.007

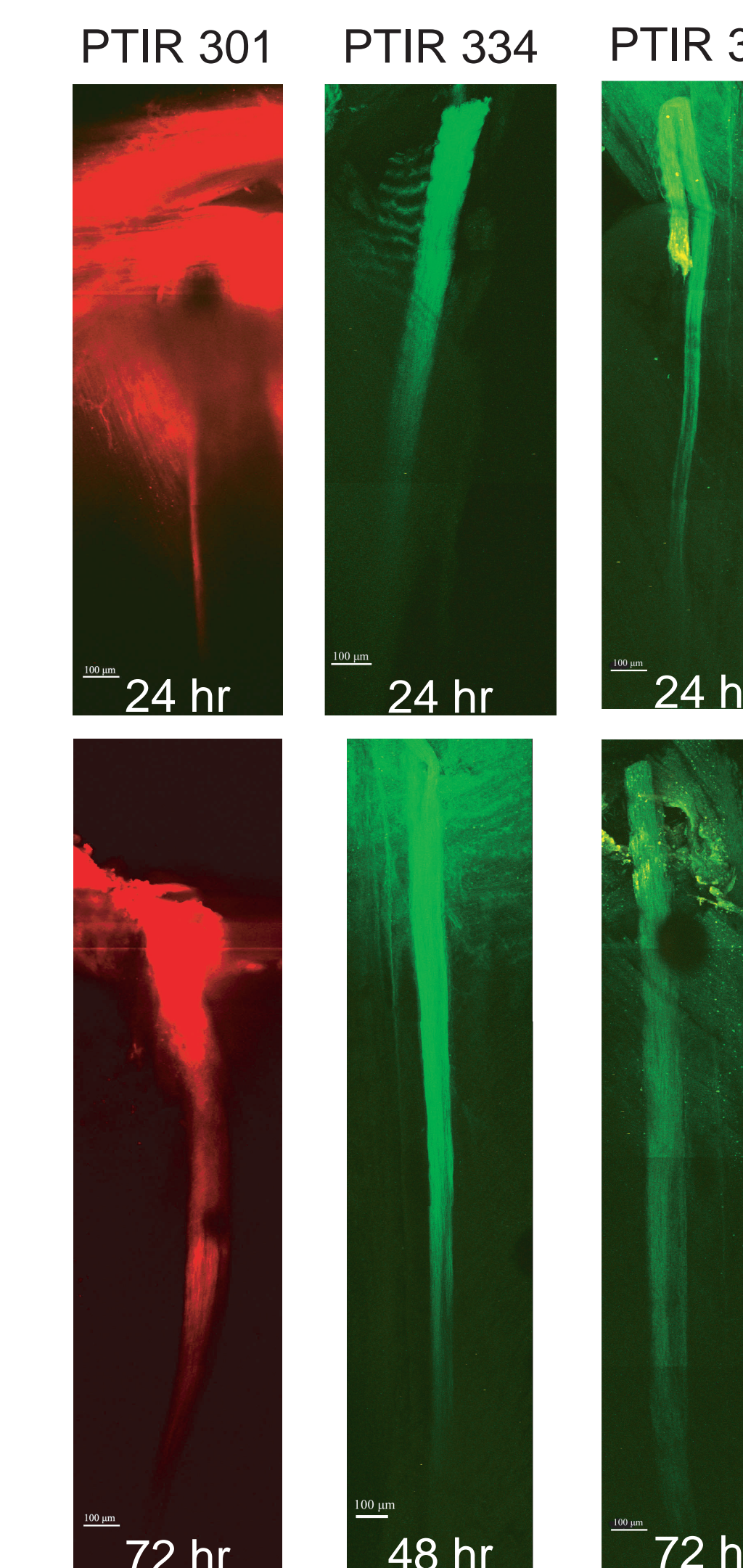


Figure 3. Peripheral nerve fiber labeling with PTIR 301 (pseudocolor red), 334 and 336 (pseudocolor green) in the mouse spinal cord model. Incubation was done at 37 C. The probes diffuse laterally from the injection site (at the top of image) along the peripheral nerve fiber towards the bottom of the image. The incubation time is given on each image. The scale bars are 100 μm .

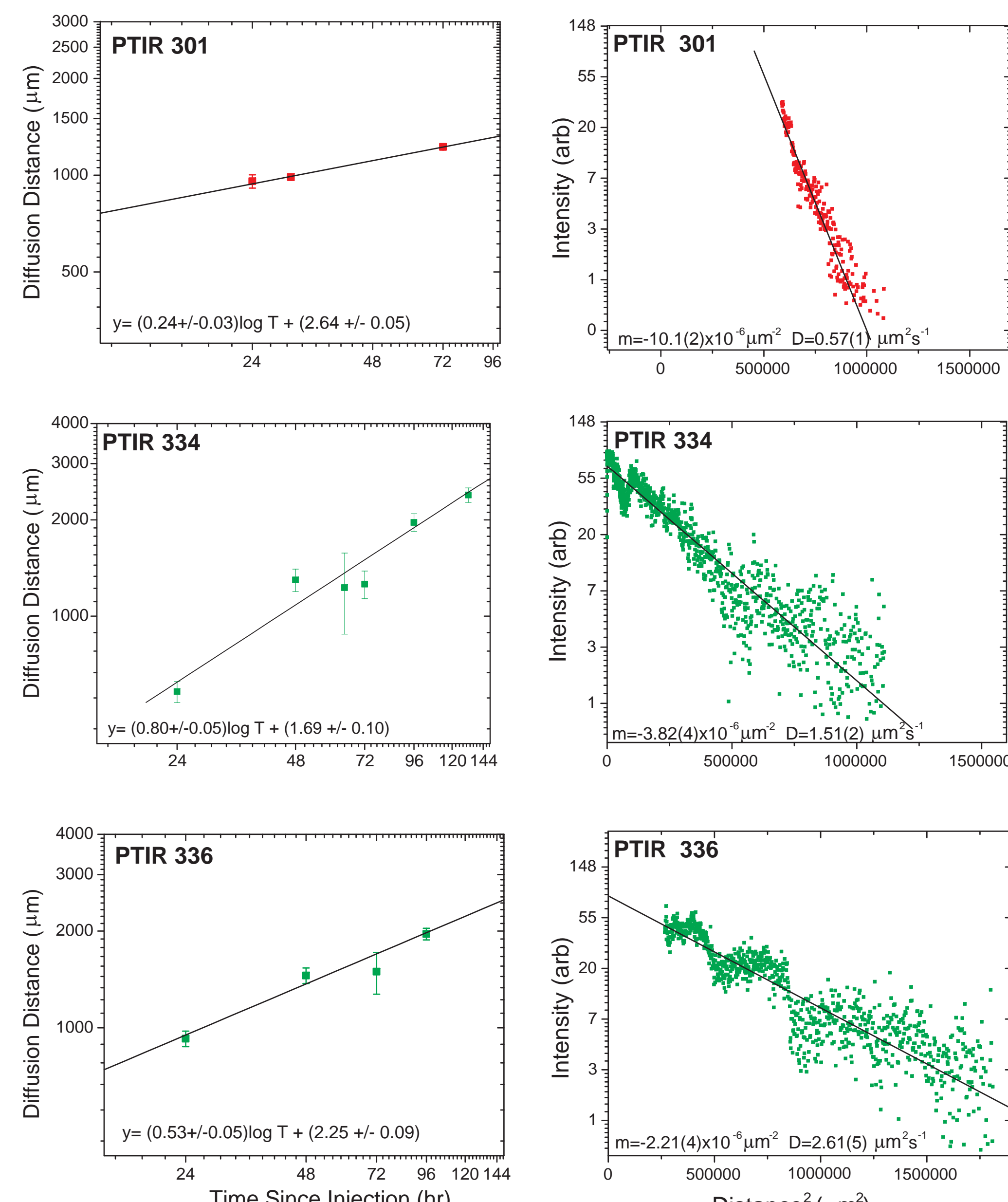


Figure 4. Diffusion distance as a function of incubation time measured for PTIR 301, 334, and 336. PTIR 336 appears to follow standard Fickian-diffusion with a time-scaling exponent of 0.53 ± 0.05 , while PTIR 301 exhibits anomalous sub-diffusion with a time-scaling exponent of 0.24 ± 0.03 , and PTIR 334 exhibits anomalous super-diffusion with an exponent of 0.80 ± 0.05 .

Figure 5. Exponential decrease in PTIR 301, 334, and 336 probe fluorescence intensity with diffusion distance along the peripheral nerve fiber after a 24 hr incubation at 37 C. The best-fit line and slope (m) are shown for each probe. The effective diffusion coefficients were calculated from the slope using Eq. 5.

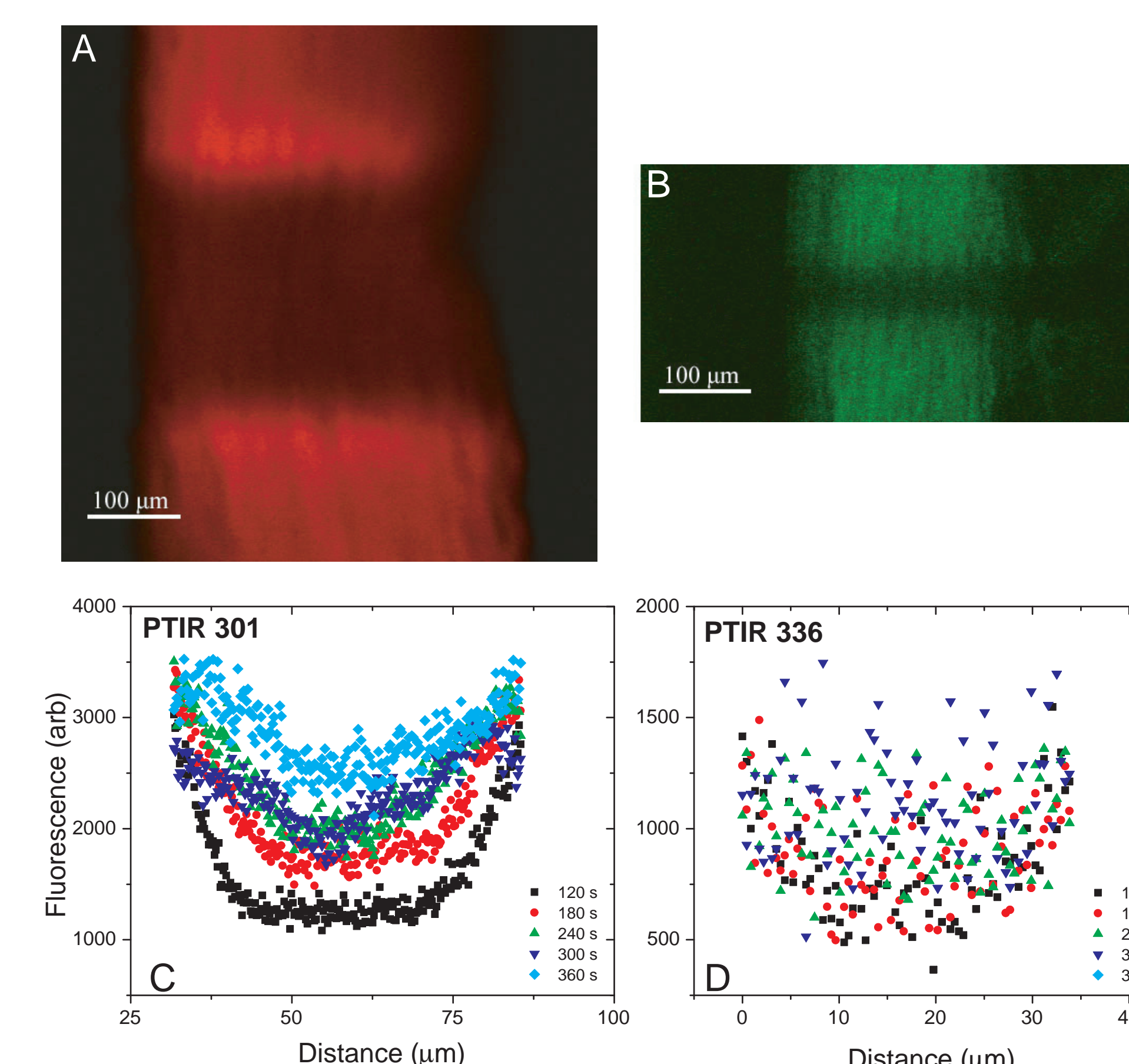


Figure 6. Fluorescence Recovery after Photobleaching (FRAP) for PTIR 301 (A,C) and 336 (B,D) labeled peripheral nerve fibers. A and B show dye fluorescence in the fiber immediately after bleaching by laser scanning at high power. Recovery following bleaching was observed over a period of several minutes. These images were analyzed to quantify the fluorescence recovery shown in C and D. Scale bars on the images are 100 μm . The results of several experiments are summarized in Table 2.

Table 2: Summary of Diffusion Measurements

	PTIR 301	PTIR 336	PTIR 334
Time-Scaling Exponent	0.24 ± 0.03	0.53 ± 0.05	0.80 ± 0.05
<i>Diffusion Coefficients ($\mu\text{m}^2/\text{s}$)</i>			
Distance - Time	4.4 ± 1.8		
Distance - Concentration	0.57 ± 0.08	0.91 ± 0.11	1.18 ± 0.43
FRAP	1.50 ± 0.29	0.12 ± 0.04	

Conclusions

- All of the candidate fluorophores can be multiphoton-excited with excitation wavelengths ranging from 720 -980 nm.
- The peaks of the two-photon action cross section spectra for Lucifer Yellow, PTIR 334, 335 and 336 are equal to, or slightly blue-shifted from what would be expected from the one-photon absorption spectra.
- In contrast NeuroVue Red exhibits a large two-photon excitation peak at 760 nm without a corresponding one-photon absorption band.
- The peak two-photon action cross sections of PTIR 334, 335 and 336 are somewhat modest, but of the same order of magnitude as other useful fluorescent probes.
- Only PTIR 336 displayed Fickian diffusion.
- PTIR 301 exhibited anomalous sub-diffusion with a time exponent of 0.24 ± 0.03 .
- PTIR 334 exhibited anomalous super-diffusion with a time exponent of 0.80 ± 0.05 .
- Variability in the measurement of the effective diffusion coefficient likely reflects the time and concentration dependence of this parameter.

References

- Jensen-Smith *et al.* Immunological Investigations , 36(5) 763-89 (2007).
- C. Xu and W. W. Webb, J. Opt. Soc. Am. B 13(3) 481-491 (1996).

Acknowledgements

This work was supported by an N.I.H. SBIR II grant MH079805, P20 RR016469 (MN) from the INBRE Program of the NCCR, and by LB692 (BF). This investigation was conducted at the Creighton University Integrated Biomedical Imaging Facility, initially constructed with support from C06 Grant RR17417-01 from the NCCR, NIH. We acknowledge Jeremy Duncan for his support in preparing the spinal cord samples.